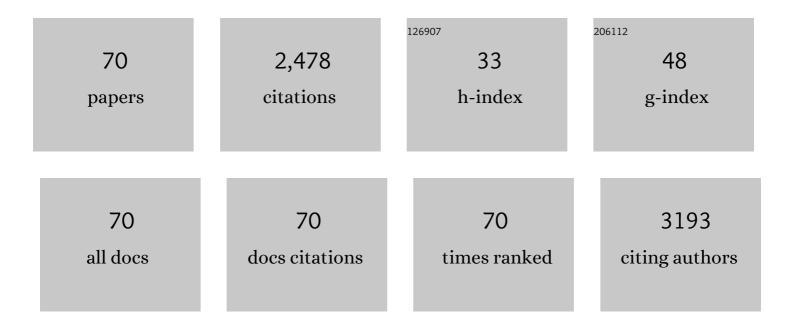
List of Publications by Year in descending order

Source: https://exaly.com/author-pdf/5510062/publications.pdf Version: 2024-02-01



YAN FENC

#	Article	IF	CITATIONS
1	An in situ gelatin-assisted hydrothermal synthesis of ZnO–reduced graphene oxide composites with enhanced photocatalytic performance under ultraviolet and visible light. RSC Advances, 2014, 4, 7933.	3.6	133
2	Two-Photon Fluorescent Probe for Monitoring Autophagy via Fluorescence Lifetime Imaging. Analytical Chemistry, 2018, 90, 7122-7126.	6.5	117
3	Electrochemical performance of graphene nanosheets and ceramic composites as anodes for lithium batteries. Journal of Materials Chemistry, 2009, 19, 9063.	6.7	109
4	A mitochondria-targeted two-photon fluorescent probe for highly selective and rapid detection of hypochlorite and its bio-imaging in living cells. Sensors and Actuators B: Chemical, 2016, 222, 483-491.	7.8	90
5	A two-photon fluorescent probe for real-time monitoring of autophagy by ultrasensitive detection of the change in lysosomal polarity. Chemical Communications, 2017, 53, 3645-3648.	4.1	85
6	Recent advances in mitochondria- and lysosomes-targeted small-molecule two-photon fluorescent probes. Chinese Chemical Letters, 2017, 28, 1943-1951.	9.0	79
7	One-pot hydrothermal synthesis of ZnS–reduced graphene oxide composites with enhanced photocatalytic properties. CrystEngComm, 2014, 16, 214-222.	2.6	71
8	Real-time visualization of autophagy by monitoring the fluctuation of lysosomal pH with a ratiometric two-photon fluorescent probe. Chemical Communications, 2019, 55, 1782-1785.	4.1	68
9	A two-photon fluorescent probe for biological Cu (â¡) and PPi detection in aqueous solution and in vivo. Biosensors and Bioelectronics, 2017, 90, 276-282.	10.1	64
10	A ratiometric two-photon fluorescent probe for hydrazine and its applications. Sensors and Actuators B: Chemical, 2015, 220, 1338-1345.	7.8	63
11	A green reduction of graphene oxide via starch-based materials. RSC Advances, 2013, 3, 21466.	3.6	62
12	A carbazole-based "turn-on―two-photon fluorescent probe for biological Cu2+ detection vis Cu2+-promoted hydrolysis. Dyes and Pigments, 2016, 125, 185-191.	3.7	60
13	Two-Photon Fluorescent Probes for Biological Mg ²⁺ Detection Based on 7-Substituted Coumarin. Journal of Organic Chemistry, 2015, 80, 4306-4312.	3.2	59
14	Preparation of reduced graphene oxide nanosheet/FexOy/nitrogen-doped carbon layer aerogel as photo-Fenton catalyst with enhanced degradation activity and reusability. Journal of Hazardous Materials, 2019, 362, 62-71.	12.4	57
15	Selective dual detection of H2S and Cu2+ by a post-modified MOF sensor following a tandem process. Journal of Hazardous Materials, 2021, 403, 123698.	12.4	55
16	A ZnS nanocrystal/reduced graphene oxide composite anode with enhanced electrochemical performances for lithium-ion batteries. Physical Chemistry Chemical Physics, 2016, 18, 30630-30642.	2.8	54
17	Electrochemical Properties of Polymerâ€Derived SiCN Materials as the Anode in Lithium Ion Batteries. Journal of the American Ceramic Society, 2009, 92, 2962-2968.	3.8	53
18	Rational design of a diaminomaleonitrile-based mitochondria – targeted two-photon fluorescent probe for hypochlorite in vivo: Solvent-independent and high selectivity over Cu2+. Sensors and Actuators B: Chemical, 2018, 254, 282-290.	7.8	53

#	Article	IF	CITATIONS
19	Design of a ratiometric two-photon fluorescent probe for dual-response of mitochondrial SO2 derivatives and viscosity in cells and in vivo. Dyes and Pigments, 2019, 171, 107709.	3.7	53
20	A rhodamine-based fluorescent probe for detecting Hg2+ in a fully aqueous environment. Dalton Transactions, 2013, 42, 14819.	3.3	48
21	Evaluation of heavy metal pollution in the sediment of Poyang Lake based on stochastic geo-accumulation model (SGM). Science of the Total Environment, 2019, 659, 1-6.	8.0	48
22	Dual-detection of mitochondrial viscosity and SO2 derivatives with two cross-talk-free emissions employing a single two-photon fluorescent probe. Sensors and Actuators B: Chemical, 2019, 297, 126777.	7.8	45
23	Preparation and improved electrochemical performance of SiCN–graphene composite derived from poly(silylcarbondiimide) as Li-ion battery anode. Journal of Materials Chemistry A, 2014, 2, 4168.	10.3	43
24	A mitochondria-targeted ratiometric two-photon fluorescent probe for biological zinc ions detection. Biosensors and Bioelectronics, 2016, 77, 921-927.	10.1	42
25	Preparation and thermal properties of hybrid nanocomposites of poly(methyl methacrylate)/octavinyl polyhedral oligomeric silsesquioxane blends. Journal of Applied Polymer Science, 2009, 111, 2684-2690.	2.6	40
26	Study on thermal enhancement mechanism of POSSâ€containing hybrid nanocomposites and relationship between thermal properties and their molecular structure. Journal of Applied Polymer Science, 2010, 115, 2212-2220.	2.6	40
27	A two-photon fluorescent probe for detecting endogenous hypochlorite in living cells. Dalton Transactions, 2015, 44, 6613-6619.	3.3	40
28	A carbazole-based mitochondria-targeted two-photon fluorescent probe for gold ions and its application in living cell imaging. Sensors and Actuators B: Chemical, 2016, 225, 572-578.	7.8	37
29	A mitochondria-targeted ratiometric two-photon fluorescent probe for detecting intracellular cysteine and homocysteine. Talanta, 2018, 178, 24-30.	5.5	37
30	One-step preparation of nanobeads-based polypyrrole hydrogel by a reactive-template method and their applications in adsorption and catalysis. Journal of Colloid and Interface Science, 2018, 527, 214-221.	9.4	36
31	Rational design of a ratiometric two-photon fluorescent probe for real-time visualization of apoptosis. Chemical Communications, 2018, 54, 10495-10498.	4.1	36
32	A mitochondria-targeted colorimetric and two-photon fluorescent probe for biological SO 2 derivatives in living cells. Dyes and Pigments, 2016, 134, 297-305.	3.7	35
33	A dual-emission two-photon fluorescent probe for specific-cysteine imaging in lysosomes and in vivo. Sensors and Actuators B: Chemical, 2019, 293, 247-255.	7.8	34
34	A mitochondrial-targeted red fluorescent probe for detecting endogenous H2S in cells with high selectivity and development of a visual paper-based sensing platform. Sensors and Actuators B: Chemical, 2020, 312, 127982.	7.8	34
35	Copper ion-mediated glyphosate detection with N-heterocycle based polyacetylene as a sensing platform. Sensors and Actuators B: Chemical, 2017, 243, 696-703.	7.8	33
36	An Efficient Heterobimetallic Lanthanide Alkoxide Catalyst for Transamidation of Amides under Solventâ€Free Conditions. Advanced Synthesis and Catalysis, 2017, 359, 302-313.	4.3	30

#	Article	IF	CITATIONS
37	Facile hydrothermal fabrication of ZnO–graphene hybrid anode materials with excellent lithium storage properties. Sustainable Energy and Fuels, 2017, 1, 767-779.	4.9	29
38	Two-dimensional carbazole-based derivatives as versatile chemosensors for colorimetric detection of cyanide and two-photon fluorescence imaging of viscosity inÂvitro. Dyes and Pigments, 2017, 137, 560-568.	3.7	24
39	Construction of bienzyme biosensors based on combination of the one-step electrodeposition and covalent-coupled sol-gel process. Science in China Series B: Chemistry, 2009, 52, 2269-2274.	0.8	22
40	A coumarin-based colorimetric and fluorescent probe for the highly selective detection of Au 3+ ions. Chinese Chemical Letters, 2016, 27, 1563-1566.	9.0	22
41	Postmodified Dual Functional UiO Sensor for Selective Detection of Ozone and Tandemly Derived Sensing of Al ³⁺ . Analytical Chemistry, 2020, 92, 11600-11606.	6.5	22
42	Accurate Monitoring and Multiple Evaluations of Mitophagy by a Versatile Two-Photon Fluorescent Probe. Analytical Chemistry, 2021, 93, 9200-9208.	6.5	22
43	Preparation and electrochemical performance of a porous polymer-derived silicon carbonitride anode by hydrofluoric acid etching for lithium ion batteries. RSC Advances, 2014, 4, 23694.	3.6	20
44	Fluorophore-Promoted Facile Deprotonation and Exocyclic Five-Membered Ring Cyclization for Selective and Dynamic Tracking of Labile Glyoxals. Analytical Chemistry, 2020, 92, 13829-13838.	6.5	18
45	pH-Independent two-photon fluorescent lysotrackers for real-time monitoring autophagy. Journal of Materials Chemistry B, 2018, 6, 1764-1770.	5.8	17
46	Strategically modified highly selective mitochondria-targeted two-photon fluorescent probe for Au3+ employing Schiff-base: Inhibited C=N isomerization vs. hydrolysis mechanism. Dyes and Pigments, 2018, 150, 241-251.	3.7	16
47	Light-driven visualization of endogenous cysteine, homocysteine, and glutathione using a near-infrared fluorescent probe. Journal of Materials Chemistry B, 2019, 7, 7723-7728.	5.8	16
48	Pendant structure governed the selectivity of Pd2+ using disubstituted polyacetylenes with sulfur functions and the application of thiophanate-methyl detection. Sensors and Actuators B: Chemical, 2017, 247, 36-45.	7.8	15
49	Design of a two-photon fluorescent probe for selective recognition of Au(III) over Au(I) and its application of imaging in vitro and in vivo. Spectrochimica Acta - Part A: Molecular and Biomolecular Spectroscopy, 2017, 187, 110-118.	3.9	14
50	Li ₂ S–Embedded copper metal–organic framework cathode with superior electrochemical performance for Li–S batteries. New Journal of Chemistry, 2018, 42, 13775-13783.	2.8	14
51	Magnetically recyclable reduced graphene oxide nanosheets/magnetite-palladium aerogel with superior catalytic activity and reusability. Journal of Colloid and Interface Science, 2017, 506, 154-161.	9.4	13
52	Design of a two-photon fluorescent probe for ratiometric imaging of endogenous hypochlorite in mitochondria. Dyes and Pigments, 2020, 181, 108548.	3.7	13
53	Oneâ€step preparation of Fe ₂ O ₃ /reduced graphene oxide aerogel as heterogeneous Fentonâ€ike catalyst for enhanced photoâ€degradation of organic dyes. ChemistrySelect, 2018, 3, 9062-9070.	1.5	12
54	Evaluating visually a new apoptosis-induced reagent by a ratiometric two-photon fluorescent pH probe. Sensors and Actuators B: Chemical, 2021, 329, 129104.	7.8	12

#	Article	IF	CITATIONS
55	The interconversion mechanism between TcO3+ and TcO2 + core of 99mTc labeled amine-oxime (AO) complexes. Theoretical Chemistry Accounts, 2008, 121, 271-278.	1.4	11
56	A novel strategy for immobilization of thionine based on calcium carbonate-gold nanoparticles inorganic hybrid composite and its application in hydrogen peroxide sensor. Science China Chemistry, 2011, 54, 545-551.	8.2	11
57	Heterobimetallic dinuclear lanthanide alkoxide complexes as acid–base bifunctional catalysts for synthesis of carbamates under solvent-free conditions. RSC Advances, 2016, 6, 78576-78584.	3.6	11
58	A lysosomal polarity-specific two-photon fluorescent probe for visualization of autophagy. Chinese Chemical Letters, 2021, 32, 1803-1808.	9.0	11
59	Real-time and accurate monitoring of mitochondria-related apoptosis by a multifunctional two-photon fluorescent probe. Sensors and Actuators B: Chemical, 2022, 351, 130953.	7.8	11
60	A simple strategy for preparation of spherical silica-supported porous chitosan matrix based on sol–gel reaction and simple treatment with ammonia solution. Analytical Methods, 2010, 2, 546.	2.7	10
61	Development of Hot-Extruded Mg–RE–Zn Alloy Bar with High Mechanical Properties. Materials, 2019, 12, 1722.	2.9	10
62	Direct activation of tachykinin receptors within baroreflex afferent pathway and neurocontrol of blood pressure regulation. CNS Neuroscience and Therapeutics, 2019, 25, 123-135.	3.9	9
63	Contribution of Baroreflex Afferent Pathway to NPY-Mediated Regulation of Blood Pressure in Rats. Neuroscience Bulletin, 2020, 36, 396-406.	2.9	7
64	Synthesis and Crystal Structure of Novel Biheterometal and Triheterometal Alkoxide Clusters – Highly Active Catalysts for the Polymerization of ϵ aprolactone. European Journal of Inorganic Chemistry, 2010, 2010, 5579-5586.	2.0	6
65	An Explosive Bombâ€Inspired Method to Prepare Collapsed and Ruptured Fe ₂ O ₃ /Nitrogenâ€Đoped Carbon Capsules as Catalyst Support. Chemistry - A European Journal, 2017, 23, 17095-17102.	3.3	6
66	An efficient and green approach to synthesizing enamines by intermolecular hydroamination of activated alkynes. Chemical Research in Chinese Universities, 2015, 31, 212-217.	2.6	4
67	Imaging of lysosomal oxidative stress during autophagy with a ratiometric probe featuring a large probe-product spectral separation. Sensors and Actuators B: Chemical, 2021, 335, 129713.	7.8	4
68	Microstructural stability of heat-resistant high-pressure die-cast Mg-4Al-4Ce alloy. International Journal of Materials Research, 2017, 108, 427-430.	0.3	2
69	Polyfluorenylacetylene for near-infrared laser protection: polymer synthesis, optical limiting mechanism and relationship between molecular structure and properties. RSC Advances, 2017, 7, 53785-53796.	3.6	1
70	Synthesis and optical properties of possâ€based oxadiazole nanohybrids with threeâ€dimensional molecular conjugated structure. Journal of Applied Polymer Science, 2014, 131, .	2.6	0